Energetics and dynamics in the reaction of Si^+ with SiF_4. Thermochemistry of SiF_x and SiF_x^+ ($x=1, 2, 3$)

M. E. Weber
Department of Chemistry, University of California, Berkeley, California 94720
P. B. Armentrout[a)]
Department of Chemistry, University of Utah, Salt Lake City, Utah 84112

(Received 9 February 1988; accepted 26 February 1988)

The title reaction is studied using guided ion beam mass spectrometry. Absolute reaction cross sections are measured as a function of kinetic energy from thermal to 40 eV, and three endothermic product channels are observed. The dominant $SiF^+ + SiF_3$ channel is only slightly endothermic, while the $SiF_3^+ + SiF$ and $SiF_2^+ + SiF_2$ channels have much higher thresholds. The SiF_3^+ cross section magnitude is about half that of SiF^+, while the SiF_2^+ cross section is an order of magnitude smaller than that of SiF^+. A second feature which appears in the SiF_2^+ cross section is due to dissociation of SiF_3^+. There is evidence that SiF^+ and SiF_3^+ are produced via a direct mechanism. Competition between these two channels is interpreted in terms of molecular orbital correlations and qualitative potential energy surfaces. One surface is found to correlate only with the $SiF_3^+ + SiF$ channel, while another correlates diabatically with this channel and adiabatically with the $SiF^+ + SiF_3$ channel. Competition on this latter surface has an energy dependence which is consistent with the Landau–Zener model. Reaction thresholds are analyzed to yield 298 K heats of formation for SiF_x and SiF_x^+ species. From an evaluation of these and literature values, we recommend the following values: $\Delta H_f^0(SiF^+) = 170.4 \pm 2.2$ kcal/mol, $IP(SiF) = 7.54 \pm 0.16$ eV, $\Delta H_f^0(SiF_3) = -258 \pm 3$ kcal/mol, and $IP(SiF_3) = 9.99 \pm 0.24$ eV.

INTRODUCTION

Silicon fluoride species and reactions involving these species have been the focus of recent theoretical[1] and experimental studies.[2–4] Such species are found in fluorine-based plasmas used to etch and deposit silicon layers in the fabrication of microelectronic devices and solar cells.[5] During etching, highly reactive fluorine radicals and ions present in the plasma bombard the surface and volatilize the silicon surface via SiF_4 [6] and SiF_2.[7,8] Deposition of silicon layers, on the other hand, involves polymerization via insertion of SiF_x species into the surface. Etching and polymerization compete, and the dominant process is determined by the physical parameters of the plasma reactor.

In recent studies of the chemistry of plasma etching and deposition, speculations have been made on the role of gas-phase ion–molecule reactions.[9–12] Such reactions have been found to rival electron-impact dissociation as a source of ion and neutral radicals,[13–15] and thereby can have a major effect on plasma composition. One example of this involves the SiH_4 plasma where the dominant ion present, SiH_3^+, is formed primarily via ion–molecule reactions.[9,16,17] It has also been proposed that gas-phase ion–molecule reactions play a direct role in deposition processes via gas-phase polymerization reactions (1), such as in a $SiCl_4/Ar$ plasma, where X = Cl[18]:

$$SiX_3^+ \xrightarrow{SiX_n} Si_2X_5^+ \xrightarrow{SiX_n} Si_xX_y^+. \quad (1)$$

Also, reaction (1), where X = H, has been investigated as a major step in the formation of undesirable hydrogenated silicon dust in silane systems.[19]

A detailed understanding of the chemical mechanisms involved in plasmas[20] can provide insight into the most important physical parameters, and benefit the development of selective etching,[6] endpoint detection,[21] and reactor design. However, much of the past work concerning plasma etching and deposition has taken an empirical approach due to the complexity of the chemistry occurring in the plasma. Such plasmas have a multitude of different ions, radicals, and neutrals which all undergo many complex chemical processes concurrently in the gas phase and at the gas–surface interface. Often the thermochemistry of many of these species and the mechanisms of the reactions are unknown. One approach to understanding the complexities of plasma chemistry involves computer modeling,[22–24] but this requires knowledge of the kinetic rates of all important reactions occurring in the plasma. While many such rates have been measured or estimated, the collection of kinetic data is not sufficient for detailed computer modeling. One reason is that most experiments measure room temperature (thermal) rate constants which are not necessarily applicable in the plasma environment. For instance, ion energies of 600 eV have been measured in rf plasmas,[6,25] and energies of 1 to 20 eV have been estimated for a dc discharge.[17] Modeling schemes must then use thermal rate constants and assume that they are independent of energy without verification. This assumption is considered to be a serious source of uncertainty.[17]

[a)] NSF Presidential Young Investigator, 1984–1989; Alfred P. Sloan Fellow; Camille and Henry Dreyfus Teacher–Scholar, 1988–1993.

 0021-9606/88/116898-13$02.10

The present work addresses these various questions by measuring the title reaction from thermal to 40 eV (50 eV in the lab frame) of kinetic energy by using guided ion beam mass spectrometry. This reaction has been investigated previously by Reents and Musjce using Fourier transform mass spectrometry (FTMS), but Si^+ was found to be unreactive toward SiF_4 at thermal energies.[3] In the present study, relative rates of ion and neutral radical production and absolute cross sections for this reaction are determined at elevated energies. These results are then analyzed to ascertain the thermochemistry of various SiF_x and SiF_x^+ species which presently have uncertainties as high as 20 kcal/mol.[26] Finally, details of the reaction mechanism are discussed.

This study is a continuation of previous work in our laboratories in which the detailed interactions of Si^+ with silane,[27] as well as Si^+,[28] SiH^+,[29] and SiD^+ [29] with dihydrogen were examined. These studies measured absolute reaction cross sections for all SiH_x^+ and $Si_2H_x^+$ product channels from thermal to 10 eV and evaluated the mechanisms of each reaction. Systematic measurements were made of the thermochemistry for comparison with previous data. Uncertainties in the resulting heats of formation are generally less than 2 kcal/mol.[27]

EXPERIMENT

The ion beam apparatus and experimental techniques used in this work are described in detail elsewhere.[30] Silicon ions are produced as described below. The $^{28}Si^+$ ions are mass analyzed and decelerated to the desired translational energy. The ion beam is injected into an rf octopole ion beam guide,[31] which passes through the reaction cell containing the SiF_4 reactant gas. The pressure of SiF_4 is maintained sufficiently low, $<2\times10^{-4}$ Torr, that multiple ion–molecule collisions are improbable. The unreacted Si^+ and product ions drift out of the gas chamber to the end of the octopole, where they are extracted and analyzed in a quadrupole mass filter. Finally, ions are detected by a secondary electron scintillation ion counter using standard pulse counting techniques. Raw ion intensities are converted to absolute reaction cross sections as described previously.[30]

The octopole beam guide utilizes rf electric fields to create a potential well which traps ions in the radial direction without affecting their axial energy.[31] One advantage of the beam guide is highly efficient product collection, and absolute cross sections as small as 10^{-3} Å^2 can be measured. In general, we estimate that the absolute uncertainty of the cross sections is $\pm 20\%$ and the relative uncertainty is $\pm 5\%$.[30] However, in this work, all silicon isotopes were not accounted for explicitly in the mass analysis of the product ions, and therefore, the absolute magnitudes may be low by up to 8% depending on the reaction mechanism.[32] Thus, the absolute uncertainty here is $\pm 30\%$. This can be even larger for charge transfer reactions, in which products may be formed through a long-range electron jump such that little or no forward momentum is transferred to the products.[33] In such a case, up to 50% of these ions may have no forward velocity in the laboratory and will not drift out of the octopole and be detected.

Laboratory ion energies (lab) are converted to energies in the center-of-mass frame (c.m.) by using the conversion $E(\text{c.m.}) = E(\text{lab})\times M/(m+M)$, where m is the ion mass and M is the target molecule mass. Unless stated otherwise, all energies quoted in this work correspond to the c.m. frame. The absolute energy scale and the corresponding full width at half-maximum (FWHM) of the ion kinetic energy distribution is determined by using the octopole beam guide as a retarding potential analyzer.[30] An accurate determination is possible since the interaction region and energy analysis region are physically the same. In this work, the uncertainty in the absolute energy scale is ± 0.04 eV and a typical FWHM is 0.5 eV. At very low energies, the slower ions in the ion beam energy distribution are not transmitted through the octopole, which results in a narrowing of the ion energy distribution. We take advantage of this effect to access very low interaction energies as described previously.[30] Energies in data plots are mean ion energies which take into account this truncation of the ion beam distribution.

Silicon ions are produced by surface ionization. In this source, a rhenium filament is resistively heated to $\sim$2200 K and is exposed to silane. The silane decomposes on the filament and ionized silicon desorbs. If the Si^+ ions equilibrate at the filament temperature, the electronic state distribution of the ions is Maxwellian.[34] Since the first excited state of Si^+ is 5.46 eV above the ground state,[35] exclusively ground state Si^+ (^2P) should be produced. A previous study has verified that no excited ions are produced by this source.[27]

RESULTS

The reaction of silicon ions with tetrafluorosilane yields four main product channels, reaction (2):

$$Si^+ + SiF_4 \rightarrow SiF^+ + SiF_3, \quad (2a)$$

$$\rightarrow SiF_3^+ + SiF, \quad (2b)$$

$$\rightarrow SiF_2^+ + SiF_2, \quad (2c)$$

$$\rightarrow SiF_2^+ + SiF + F. \quad (2d)$$

Their reaction cross sections σ are shown as a function of relative translational energy in Fig. 1. The results shown are the average of ten data sets taken under different experimental conditions over the course of five months. The behavior of each cross section is characteristic of an endothermic reaction, since they rise rapidly from an energy threshold. Despite a careful search, the present work found no other product ions, such as $Si_2F_x^+$, at any energy. This means that the cross section for such species must be less than 10^{-3} Å^2. These results explain why no reaction was observed by Reents and Musjce.[3] In their study, measurements could be made only at the reaction temperature of $\sim$400 K ($3kT/2 \simeq 0.05$ eV) which is below the apparent thresholds of all reaction channels.

The predominant product ion is SiF^+, process (2a). This channel is slightly endothermic, and its cross section rises as $E^{1.6\pm0.1}$, until $\sim$5 eV. It then exhibits a slight but reproducible change in behavior such that above 5 eV, the cross section behaves as $E^{1.0\pm0.1}$. It continues to rise until $\sim$9 eV, where it reaches a maximum cross section of 1.2 Å^2.

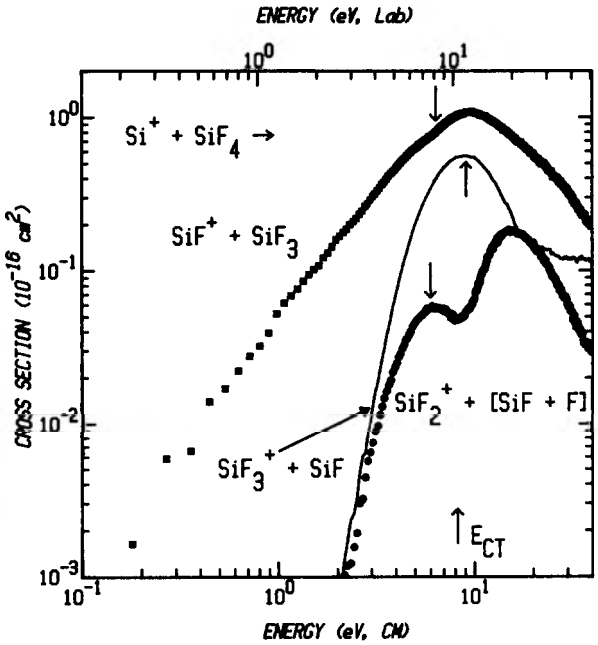

FIG. 1. Variation of SiF_x^+ product cross sections with translational energy in the laboratory frame of reference (upper scale) and the center-of-mass frame (lower scale) for reaction (2). SiF^+ (squares) and SiF_3^+ (line) cross sections result from reactions (2a) and (2b), respectively. The first feature in the SiF_2^+ cross section (circles) corresponds to reaction (2c) with SiF_2 as the neutral product, while the second feature corresponds to reaction (2d) with the dissociated products SiF and F. The arrow marked E_{CT} indicates the thermodynamic threshold for the charge transfer process (8b). The arrows at 6.4, 9.1, and 6.0 eV (top to bottom) show the thermodynamic thresholds for the dissociative processes (7a), (7b), and (7c), respectively.

Beyond this maximum, in the energy range of 13 to 30 eV, $\sigma(SiF^+)$ falls off as $E^{-1.3\pm0.3}$.

The SiF_3^+ cross section, reaction (2b), is also endothermic, but the apparent threshold of ~2 eV lies much higher than that of SiF^+. The SiF_3^+ channel also peaks at ~9 eV and its cross section is about half $\sigma(SiF^+)$ in magnitude, 0.6 Å^2, at this energy. The SiF_3^+ cross section then decreases as $E^{-2.5\pm0.4}$ until ~18 eV. Beyond this energy, the cross section levels off and behaves as $E^{-0.5\pm0.6}$. This change in behavior at high energies implies that a new process for production of SiF_3^+ has become available.

The final product channel observed is SiF_2^+, process (2c), and it shows markedly different behavior. Specifically, the cross section comprises two features. The first shows an apparent endothermicity of ~2 eV and a maximum cross section at ~6 eV. This maximum is an order of magnitude smaller and occurs 3 eV lower than that for the SiF^+ and SiF_3^+ channels. At higher energies, there is a second and dominant feature, which has an estimated onset of ~8 eV. This feature coincides with the decline of the SiF_3^+ channel, which suggests that this feature may correspond to dissociation of the SiF_3^+ product into SiF_2^+ and F, reaction (2d). The second feature in the SiF_2^+ cross section reaches a maximum value of 0.2 Å^2 at ~16 eV. Beyond this energy the SiF_2^+ cross section decreases as $E^{-2.7\pm0.5}$.

One of the more interesting features in these cross sections is the change in the slope of $\sigma(SiF^+)$ at about 5 eV. This change cannot be due to dissociation of SiF^+, since this process is not energetically accessible until 6.4 eV. An alternate explanation is that other product channels begin to compete efficiently with SiF^+ at this energy. Based on the size of the cross sections, we surmise that this must be formation of $SiF_3^+ + SiF$ which has a cross section that is 30% of the $\sigma(SiF^+)$ magnitude at 5 eV. Direct competition between reactions (2a) and (2b) is reasonable since the only difference between the $SiF^+ + SiF_3$ and $SiF_3^+ + SiF$ channels is the location of the odd electron.

Threshold behavior

The threshold regions of endothermic reactions are analyzed using the empirical model, Eq. (3),

$$\sigma(E) = \sigma_0(E - E_T)^n/E^m, \tag{3}$$

where E_T is the translational threshold energy, σ_0 is an energy independent scaling factor, and n and m are variable parameters. This general form has been discussed previously.[36,37] In this study, we have chosen to restrict the values of m to 0, 1, and 3. A value of $m = 1$ is chosen because this form of Eq. (3) has been derived by Chesnavich and Bowers as a model for translationally driven reactions.[38] Furthermore, with $m = 1$, Eq. (3) has been found to be quite useful in describing the shapes of endothermic reaction cross sections and in deriving accurate thermochemistry from the threshold energies E_T for a wide range of systems. These systems include similar reactions, such as $Si^+ + SiH_4$,[27] as well as reactions of atomic transition metals with H_2, D_2,[34] and hydrocarbons.[37] Data analyses which use Eq. (3) with $m = 0$ and $m = 3$ are included because these models provide reasonable upper and lower limits to E_T, respectively.

For a given value of m, the other parameters σ_0, E_T, and n are optimized by using nonlinear least-squares regression analysis to give the best fit to the data, after convoluting over the known ion beam and neutral energy distributions.[30] The data is fit from below threshold up to energies where competitive processes, such as dissociation, can begin to decrease the reaction cross section. This maximum energy is 4 eV for SiF^+, 5 eV for SiF_2^+, and 6 eV for SiF_3^+ cross sections. Four

TABLE I. Optimum parameters for threshold fits.

Reaction products	m	n	E_T (eV)	Average E_T (eV)
$SiF^+ + SiF_3$	0	1.51 ± 0.05	0.16 ± 0.04	0.10 ± 0.05
	1	2.50 ± 0.05	0.09 ± 0.02	
	3	4.49 ± 0.06	0.05 ± 0.01	
$SiF_3^+ + SiF$	0	1.86 ± 0.13	2.66 ± 0.12	2.48 ± 0.14
	1	2.46 ± 0.15	2.52 ± 0.11	
	3	3.81 ± 0.20	2.27 ± 0.11	
$SiF_2^+ + SiF_2$	0	1.35 ± 0.09	2.47 ± 0.12	2.35 ± 0.12
	1	1.85 ± 0.15	2.38 ± 0.11	
	3	3.00 ± 0.25	2.19 ± 0.1	

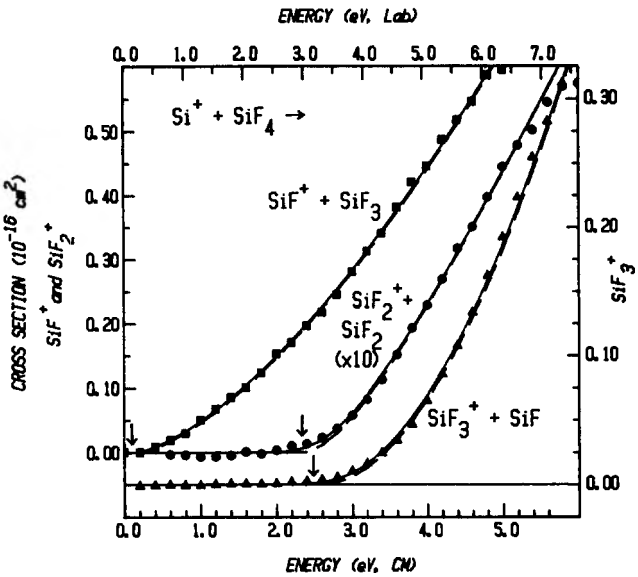

FIG. 2. Threshold regions of the SiF_x^+ product cross sections from reactions (2a, squares), (2b, triangles), and (2c, circles). The left-hand vertical scale corresponds to the SiF^+ and SiF_2^+ product ions, although SiF_2^+ has been enlarged here by a factor of 10. The right-hand vertical scale corresponds to the SiF_3^+ product ion. The dashed lines show the $m = 1$ threshold model given in Eq. (3), with the optimized n values and the recommended threshold energies E_T shown in Table I. The arrows indicate these threshold energies. The solid lines show the threshold models convoluted over the ion beam and neutral energy distributions.

data sets taken at different times and under different experimental conditions are analyzed. An average value of n (for a given m) is determined for each product channel, and then each n and m pair is used to find a optimum value of E_T for each data set. The average of these values for E_T are reported in Table I along with the optimum n values for each m. The uncertainties in E_T reported here include one standard deviation of the average value and the absolute uncertainty in our energy scale, 0.04 eV.

The best value for E_T is chosen as the average of all three model functions and is 0.10 ± 0.05 eV for reaction (2a); 2.48 ± 0.14 eV for reaction (2b); and 2.35 ± 0.12 eV for reaction (2c). Figure 2 shows the threshold fits with these thresholds, $m = 1$, and n equal to the optimized n for each channel. Very good agreement is found between these fits and the experimental data. For all three channels, there is little difference between the unconvoluted form of Eq. (3) and that convoluted over the experimental energy distributions.

As mentioned above, a form of Eq. (3) with $m = 1$ is predicted by a model for translationally driven reactions.[38] This model predicts that the value of n is given by Eq. (4),

$$n = (\Delta v + 2)/2, \tag{4}$$

where Δv is the change in the number of vibrational degrees of freedom upon formation of the intermediate from reactants. For channels (2a), (2b), and (2c), all possible reaction intermediates have six atoms and therefore $v = 12$.

TABLE II. Heats of formation at 298 K (kcal/mol).

	This work	JANAF[a]	Walsh[b]	Other[c]	Recommended
Si		107.6 (1.9)			107.6 (1.9)
SiF		− 4.8 (3)	− 5 (6)		− 5 (3)
SiF_2	− 142.4 (1.6)	− 141 (3)	− 141 (2)		− 141 (2)
SiF_3	− 257.0 (2.7)	− 259.4 (4)	− 239 (5)	− 259.4 (4.0)[d]	− 258 (3)
				− 250[e]	
				− 247[f]	
				− 253 (14)[g]	
				− 235 (20)[g]	
				− 237 (1)[h]	
SiF_4		− 386.0 (0.2)	− 386.0 (0.2)		− 386.0 (0.2)
Si^+		− 297.1 (1.0)			− 297.1 (1.0)
SiF^+	170.4 (2.2)			172[f]	170.4 (2.2)
SiF_2^+	106 (4)[i]				109 (2)
	107.6 (2.0)[j]				
SiF_3^+	− 26.7 (4.5)			− 30 (7)[g]	− 26.2 (4.7)
				− 22 (5)[e]	
				− 16[k]	

[a] Reference 39.
[b] Reference 40.
[c] Ion heats of formation calculated from literature IP values (Table III) are not included here.
[d] Reference 43.
[e] Reference 48.
[f] Reference 1.
[g] Reference 47.
[h] Reference 54.
[i] Calculated assuming literature value for $\Delta H_f^0(SiF_2)$.
[j] Calculated by assuming literature value for $IP(SiF_2)$.
[k] Reference 51.

Since $\nu(SiF_4) = 9$ and $\nu(Si^+) = 0$, Eq. (4) leads to a predicted value for n equal to 2.5 for all three channels. Experimentally, we find that when $m = 1$, the optimum value of n for the SiF^+ and SiF_3^+ channels are both very close to this value, namely 2.50 ± 0.05 and 2.46 ± 0.15, respectively. For the SiF_2^+ channel, on the other hand, the optimum value of n is 1.85 ± 0.20. The significance of this is discussed below.

DISCUSSION

Thermochemistry

Literature thermochemistry for SiF_x and SiF_x^+ species are given in Tables II and III. Heats of formation for Si^+ and SiF_4 are well known.[39,40] Values for SiF_x radicals come from two recent reviews of the literature thermochemistry by Walsh[40] and in the JANAF tables.[39] Their recommended values are in agreement for $\Delta H_f^0(SiF)$ and $\Delta H_f^0(SiF_2)$, but the values for $\Delta H_f^0(SiF_3)$ conflict by 20 kcal/mol. Values for SiF_x^+ are much less well known.

To more firmly establish this thermochemistry, heats of formation for both ion and neutral SiF_x species can be calculated from the endothermicities of reactions (2a), (2b), and (2c) listed in Table I. These calculations must assume that there are no energy barriers in excess of the true endothermicity of the reaction; however, this assumption is often quite reasonable for ion–molecule reactions since the long-range ion-induced dipole attraction eliminates small energy barriers.[41] In the strictest sense, the heats of formation derived by using this assumption are upper limits to the true values. There is also some ambiguity concerning the temperature of the products at threshold.[37] We assume here that, except for the kinetic energy of the reactant Si^+, all reactants and products are characterized by a temperature of 298 K, the nominal temperature of the reactant SiF_4. Also, we calculate ion heats of formation by using the convention that the electron is a monatomic gas. Values from the literature which use the "stationary electron" convention have been increased by 1.48 kcal/mol at 298 K.

TABLE III. Ionization potentials (eV).

	This work	Literature	Recommended
Si		8.152[a]	8.152
SiF	7.54 (0.16)	7.26[b]	7.54 (0.16)
		7.5 (0.4)[c]	
		7.4 (0.1)[d]	
SiF_2	10.65 (0.2)[e]	10.78 (0.05)[f]	10.78 (0.05)
		11.29 (0.3)[g]	
		11.0 (0.05)[c]	
		10.7 (0.2)[h]	
SiF_3	9.92 (0.26)	9.86[i]	9.99 (0.24)
		9.6 (0.6)[j]	

[a]Reference 35.
[b]Reference 46.
[c]Reference 42.
[d]Reference 2(a).
[e]Calculated assuming literature value for $\Delta H_f^0(SiF_2)$.
[f]Reference 55.
[g]Reference 47.
[h]Estimated adiabatic IP from Ref. 56.
[i]Reference 48.
[j]Reference 2(b).

SiF. The average heat of formation for SiF from two independent studies is -5 ± 3 kcal/mol.[42,43] This value is essentially adopted by both Walsh and the JANAF tables, although Walsh recommends a larger uncertainty, 6 kcal/mol. As we shall see, use of this value results in a self-consistent set of thermochemistry. We therefore find no reason to doubt its accuracy at present.

SiF^+. While our studies of reaction (2a) can provide thermochemical data for SiF^+, this requires the heat of formation of SiF_3, which is poorly characterized. Instead we have chosen to measure $\Delta H_f^0(SiF^+)$ via an independent reaction, process (6):

$$Si^+ + BF_3 \rightarrow SiF^+ + BF_2. \qquad (6)$$

In preliminary studies, we have measured a threshold energy for this reaction of $E_T = 0.16 \pm 0.07$ eV.[44] The heats of formation for BF_3 [39] and BF_2 [45] are well known to be -271.41 ± 0.41 and -141.0 ± 1.0 kcal/mol, respectively. Together, these values provide $\Delta H_f^0(SiF^+) = 170.4 \pm 2.2$ kcal/mol which yields $D^0(SiF^+) = 6.32 \pm 0.11$ eV. This is in good agreement with a theoretical value of 6.25 eV,[1] which leads to $\Delta H_f^0(SiF^+) = 172$ kcal/mol.

When our value for $\Delta H_f^0(SiF^+)$ is combined with the heat of formation of SiF given above, the ionization potential (IP) of SiF is found to be 7.54 ± 0.16 eV. This IP can be compared with several literature values. Johns and Barrow (JB) have determined a value of 7.26 eV using a Rydberg analysis.[46] However, in the same study, JB determined a value for the IP of the isovalent molecule CF which is 0.29 eV lower than the currently accepted value.[39] If a similar error is present for SiF, then IP(SiF) should be closer to $7.26 + 0.29 = 7.55$ eV. Two electron impact studies support this higher value. Ehlert and Margrave measured IP(SiF) to be 7.5 ± 0.4 eV,[42] while Freund and co-workers report a value of 7.4 ± 0.1 eV.[2(a)] Based on these comparisons, we recommend 170.4 ± 2.2 kcal/mol for $\Delta H_f^0(SiF^+)$, 7.54 ± 0.16 eV for IP(SiF), and 6.32 ± 0.11 eV for $D^0(SiF^+)$.

SiF_3^+. From the threshold energy of reaction (2b), $\Delta H_f^0(SiF_3^+)$ is determined to be -26.7 ± 4.5 kcal/mol. This value can be compared with two previous measurements. First, Margrave and co-workers measured the appearance potential of SiF_3^+ from SiF_4 as 16.2 ± 0.3 eV.[47] This leads to a value for $\Delta H_f^0(SiF_3^+)$ of -30 ± 7 kcal/mol. Second, Murphy and Beauchamp have measured a photoionization threshold for SiF_3^+ from CH_3SiF_3,[48] which leads to $\Delta H_f^0(SiF_3^+) = -22 \pm 5$ kcal/mol.[49] The average of these three values is -26.2 ± 4.7 kcal/mol (with pooled error)[50] and is our recommended heat of formation. When this heat of formation is combined with $\Delta H_f^0(SiF_4)$ and $\Delta H_f^0(F^-) = -61.0 \pm 0.1$ kcal/mol,[39] it yields $D^0(SiF_3^+ - F^-) = 299 \pm 5$ kcal/mol which can be compared with a calculated value of 309 kcal/mol.[51]

SiF_3. Having ascertained $\Delta H_f^0(SiF^+)$, we can use the

threshold energy of reaction (2a) to determine a value for $\Delta H_f^0(SiF_3)$ of -257.0 ± 2.7 kcal/mol. This value is in good agreement with a measurement by Farber and Srivastava (FS),[43] $\Delta H_f^0(SiF_3) = -259.4 \pm 4.0$ kcal/mol, which has been adopted in the JANAF tables. It also agrees reasonably well with an estimate by Murphy and Beauchamp of -250 kcal/mol.[48] Garrison and Goddard calculate $D^0(F\text{–}SiF_3) = 6.53$ eV but estimate that the true value is ~6.8–6.9 eV.[1] These bond energies can be used to yield $\Delta H_f^0(SiF_3) = -254$ kcal/mol and estimated values of ~ -247 kcal/mol. Finally, our value agrees with an experimental value reported by Margrave and co-workers, $\Delta H_f^0(SiF_3) = -253 \pm 14$ kcal/mol.[47] They changed this value to $\Delta H_f^0(SiF_3) = -235 \pm 20$ kcal/mol based on an unpublished theoretical value for $IP(SiF_3) = 8.5 \pm 1$ eV.[47] We can reproduce neither of these values from the appearance potentials given in the paper. Based on this and the very large error limits in the calculated IP, we discount this work.

Further support for our heat of formation comes from determinations of the ionization potential of SiF_3. This has been estimated as 9.86 eV by Murphy and Beauchamp,[48] and measured from electron impact studies by Freund and coworkers to be 9.6 ± 0.6 eV.[2(b)] These values, in conjunction with $\Delta H_f^0(SiF_3^+)$, result in $\Delta H_f^0(SiF_3) = -255$[48] and -249 ± 14 kcal/mol, respectively. When our values for $\Delta H_f^0(SiF_3)$ and $\Delta H_f^0(SiF_3^+)$ are combined, we derive $IP(SiF_3) = 9.92 \pm 0.26$ eV.

A conflicting value for $\Delta H_f^0(SiF_3)$ comes from work of Walsh and Doncaster, who used a kinetic iodination technique[52] to derive the bond energy $D^0(H\text{–}SiF_3) = 100.1 \pm 1.2$ kcal/mol. When coupled with $\Delta H_f^0(HSiF_3) = -287 \pm 5$ kcal/mol, this provides Walsh's recommended value of $\Delta H_f^0(SiF_3) = -239 \pm 5$ kcal/mol.[40] This is in agreement with recent *ab initio* calculations on heats of reaction for isodesmic reactions[53] which provide a value for $\Delta H_f^0(SiF_3)$ of -237 ± 1 kcal/mol.[54] However, Farber and Srivastava have measured $\Delta H_f^0(HSiF_3)$ as -293 ± 2 kcal/mol,[43] suggesting that $\Delta H_f^0(SiF_3) = -245 \pm 3$ kcal/mol. The remaining discrepancy with our work could lie in the values for $\Delta H_f^0(HSiF_3)$ or $D^0(H\text{–}SiF_3)$, neither of which seems particularly well established.

If the true value of $\Delta H_f^0(SiF_3)$ were -239 ± 5 kcal/mol, then the threshold energy for reaction (2a) should be 0.88 ± 0.24 eV, 0.78 ± 0.25 eV higher than we observe. While it is possible that a measured reaction threshold can be too high due to activation barriers, it is not possible for it to be too low in the present case. While the 0.78 eV error could be compensated by a comparable error in $\Delta H_f^0(SiF^+)$, this value seems relatively secure and is unlikely to be in error by 0.78 eV (18 kcal/mol). We therefore recommend $\Delta H_f^0(SiF_3) = -258 \pm 3$ kcal/mol, which is the average of our value and that from FS. This value when combined with $\Delta H_f^0(SiF_3^+)$ yields our recommended $IP(SiF_3) = 9.99 \pm 0.24$ eV.

SiF_2 and SiF_2^+. From the threshold energy of reaction (2c), we find the value for the sum of $\Delta H_f^0(SiF_2^+)$ and $\Delta H_f^0(SiF_2)$ to be -34.7 ± 3.0 kcal/mol. The value for $\Delta H_f^0(SiF_2)$ seems well established in the literature as -141 ± 2 kcal/mol.[39,40] Using this value, we obtain $\Delta H_f^0(SiF_2^+) = 106 \pm 4$ kcal/mol which then yields $IP(SiF_2) = 10.65 \pm 0.2$ eV. Several values for $IP(SiF_2)$ are given in the literature. Westwood determined a value of 10.78 ± 0.05 eV from photoelectron spectra (PES).[55] This value is supported in two studies by Margrave and co-workers, where the appearance potential of SiF_2^+ from SiF_2 is measured as 11.29 ± 0.3 [47] and 11.0 ± 0.05 eV.[42] The PES of SiF_2 has also been measured by Fehlner and Turner but they provide only a value for the vertical IP of 11.08 eV.[56] We estimate the adiabatic $IP(SiF_2)$ as 10.7 ± 0.2 eV from their published spectra, again in agreement with Westwood. By assuming the literature value for $IP(SiF_2) = 10.78 \pm 0.05$ eV instead of $\Delta H_f^0(SiF_2)$, we derive from our results that $\Delta H_f^0(SiF_2) = -142.4 \pm 1.6$ kcal/mol and $\Delta H_f^0(SiF_2^+) = 107.6 \pm 2.0$ kcal/mol. Overall, the thermochemistry is self-consistent. Therefore, we recommend $\Delta H_f^0(SiF_2) = -141 \pm 2$ kcal/mol, $IP(SiF_2) = 10.78 \pm 0.05$ eV, and $\Delta H_f^0(SiF_2^+) = 109 \pm 2$ kcal/mol.

Reaction mechanisms

Insight into the reaction mechanisms for processes (2) is obtained from a comparison of the observed cross sections to those calculated from phase space theory (PST).[57] PST is a statistical theory, and should apply to reactions which

TABLE IV. Parameters used in phase space theory calculations.

	$Si^+ + SiF_4$	$SiF^+ + SiF_3$	$SiF_3^+ + SiF$	$SiF_2^+ + SiF_2$
ν[a] (cm^{-1})	801	900	600	770
	264 (2)	832	560	340
	1030 (3)	406	940 (2)	1100
	389 (3)	954 (2)	320 (2)	855
		290 (2)	857	345
				872
B[a] (cm^{-1})	0.138	0.59	1.92	0.4
		2.05	0.581	0.409
α[b] (Å^3)	3.32	3.05	1.32	2.35
μ[c] (amu)	22.05	30.28	30.28	32.99
E (eV)	0	0.10	2.48	2.35
s[d]	12	3	3	4
G[e]	6	2	4	2
g_1[f]	2	2	2	2
g_2[f]	2	0	2	0

[a]Vibrational frequencies and molecular rotational constants for neutral species were taken from Ref. 39. Those for the ions were estimated by comparison to SiF_x, CF_x, and CF_x^+ constants (Ref. 39). Constants for SiCl and $SiCl^+$ [Y. Nishimura and T. Mizuguchi, J. Chem. Phys. **78**, 7260 (1983)] verified these estimations. The constants for ionic species are listed first. Vibrational degeneracies are given in parentheses.

[b]SiF and SiF_3 polarizabilities were calculated empirically [K. J. Miller and J. A. Savchik, J. Am. Chem. Soc. **101**, 7206 (1979)] using the SiF_4 [E. W. Rothe and R. B. Bernstein, J. Chem. Phys. **31**, 1619 (1959)] and SiF_2 [E. R. Lippincott, G. Nagarajan, and J. M. Stutman, J. Phys. Chem. **70**, 78 (1966)] polarizabilities.

[c]Reduced mass.

[d]Product of symmetry numbers.

[e]Total number of electronic surfaces. See Ref. 70.

[f]Number of surfaces energetically accessible to the intermediate complex. Case 1 involves reaction along the A' surface, while case 2 involves the A'' surface. See the discussion in the text. Final results shown in Fig. 3 are the sum of these two cases.

form a long-lived intermediate with strong coupling. Previous studies in our laboratories have demonstrated such intimate behavior in atom–diatom ion–molecule reactions through the ability of phase space theory to reproduce reaction cross sections as a function of energy in both shape and magnitude.[34,58] Phase space calculations were performed here by adapting programs provided recently by Chesnavich, which are described elsewhere.[59] Molecular parameters for reaction (2) necessary to perform PST calculations are given in Table IV.

The cross sections calculated using PST, σ_{PST}, are presented in Fig. 3 along with versions convoluted over the experimental energy distributions.[30] These cross sections show markedly different behavior than those observed. For instance, $\sigma(SiF^+)_{PST}$ rises far more rapidly than the observed cross section, peaks at very low energies, and then behaves as $E^{-0.5}$ until channels (2b) and (2c) begin to compete with SiF^+ production. In this region, $\sigma(SiF^+)$ is about one-half the collision cross section $\sigma_L = \pi e(2\alpha/E)^{0.5}$.[60] The PST cross section for SiF_2^+ also rises far more rapidly above the threshold region than that observed. In fact, at ~5.5 eV, $\sigma(SiF_2^+)_{PST}$ equals $\sigma(SiF^+)_{PST}$ and exceeds the experimental $\sigma(SiF_2^+)$ by nearly two orders of magnitude. In the case of the $SiF_3^+ + SiF$ channel, however, the calculated cross section is *smaller* than the observed $\sigma(SiF_3^+)$ by almost an order of magnitude. In each case, the shapes of the calculated and observed cross sections differ significantly. These discrepancies between PST calculations and experimental observations imply that the reaction dynamics inhibit SiF^+ and SiF_2^+ formation, yet enhance SiF_3^+ formation. Apparently, direct rather than statistical mechanisms are involved in one or more reaction channels.

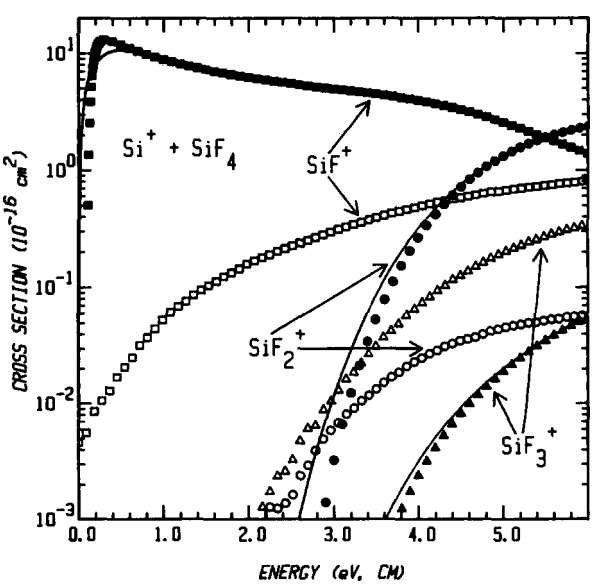

FIG. 3. Cross sections calculated using phase space theory (solid symbols) vs those observed (open symbols) as a function of translational energy in the center-of-mass frame. The solid lines show the calculated cross sections convoluted over the ion beam and neutral energy distributions.

Evidence for a direct mechanism in which the SiF^+ and SiF_3^+ channels are coupled is provided by the shapes of the threshold regions. As discussed above, the optimized form of Eq. (3) with $m = 1$ corresponds to the prediction of the translationally driven reaction model[38] for the SiF^+ and SiF_3^+ channels. Also, the break in the SiF^+ cross section at ~5 eV can be explained as competition from the SiF_3^+ cross section, implying that these two processes are coupled. A logical mechanism to produce SiF_3^+ and SiF^+ involves interaction of the Si^+ with a single F atom of SiF_4, followed by cleavage of the F–SiF_3 bond. If homolytic cleavage occurs, $SiF^+ + SiF_3$ are formed, while heterolytic cleavage produces $SiF_3^+ + SiF$. Such a mechanism is indeed direct and couples reactions (2a) and (2b).

For reaction (2c), the optimized form of Eq. (3) with $m = 1$ results in a value of n different than the model for translationally driven reactions. This implies that a separate mechanism produces SiF_2^+. The fact that the first feature in $\sigma(SiF_2^+)$ is an order of magnitude smaller than $\sigma(SiF^+)$ and $\sigma(SiF_3^+)$, implies that the SiF_2^+ reaction mechanism must be much less favored. There are two possible mechanisms for SiF_2^+ production. One plausible mechanism involves insertion of Si^+ into the F–SiF_3 bond to form intermediate I, followed by F migration to form intermediate II.

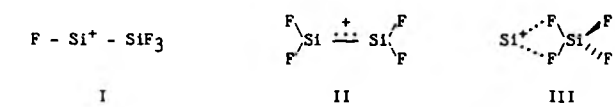

Si–Si bond cleavage then results in reaction (2c). If either the first, second, or third step were hindered, then such a mechanism would explain the small size of the SiF_2^+ cross section. Also note that if I breaks apart prior to F transfer, then $SiF^+ + SiF_3$ or $SiF_3^+ + SiF$ will be formed in preference to reaction (2c). Another possible mechanism is where the Si^+ approaches the SiF_4 in C_{2v} symmetry to form intermediate III. Abstraction of the two F atoms then yields channel (2c). As the symmetry of III relaxes from C_{2v}, then the interaction becomes more like the collinear reaction geometry which yields SiF^+. Thus if intermediate III is responsible for SiF_2^+ production, then the geometry of Si^+ approach which leads to formation of SiF_2^+ is very restricted. This would also explain the small magnitude of $\sigma(SiF_2^+)$ relative to $\sigma(SiF^+)$ and $\sigma(SiF_3^+)$.

No disilicon species are observed, in contrast to the $Si^+ + SiH_4$ system.[27,61] This may imply that intermediates I and II are unlikely. If they are formed, dissociation of the Si–Si bond must be preferred over dissociation of Si–F bonds or loss of F_2. Si–Si dissociation is thermodynamically favored, since the average silicon–fluorine bond is 5.9 ± 0.3 eV, while the average silicon–silicon bond energy is only 3.9 ± 0.8 eV.[62] The absence of disilicon products demon-

strates that polymerization of silicon in a SiF_4 plasma does not proceed through gas-phase ion–molecule reactions.

High-energy behavior

At high kinetic energy, the excess energy available to the products must go either into translation or into internal modes of the neutral or ionic species. If enough energy lies in the internal modes of the SiF_x^+ product, then the product ions will dissociate as in processes (7):

$$Si^+ + SiF_4 \rightarrow SiF^+ + SiF_3 \rightarrow Si^+ + F + SiF_3, \quad E_D = 6.4 \text{ eV}, \tag{7a}$$

$$\rightarrow SiF_3^+ + SiF \rightarrow SiF_2^+ + F + SiF, \quad E_D = 9.1 \text{ eV}, \tag{7b}$$

$$\rightarrow SiF_2^+ + SiF_2 \rightarrow SiF^+ + F + SiF_2, \quad E_D = 6.0 \text{ eV}. \tag{7c}$$

Here, the first step in each process corresponds to reactions (2a), (2b), and (2c), while the overall reaction (7b) is the same as reaction (2d). The values of E_D shown are the thermodynamic thresholds for the overall processes. These values are the sum of the corresponding bond dissociation energies and reaction threshold energies E_T, calculated with the recommended thermochemistry given above.

We can compare the thresholds for these high-energy processes, shown as arrows in Fig. 1, to the observed behavior of the reaction cross sections. A given cross section will peak and begin to fall off at the dissociation threshold E_D if a fraction of the products are formed with all of the excess energy in the internal modes of the ion. Whether this occurs depends on the reaction mechanism, and thus the locations of the peaks in the cross sections can provide mechanistic information.

For SiF^+, process (2a), the cross section peaks ~ 3 eV above E_D [reaction (7a)]. One explanation for this delay is that the excess energy is channeled into the internal modes of the SiF_3 neutral species, rather than the product ion. This is likely since SiF_3 has many low frequency vibrations, while SiF^+ has a much higher frequency vibration, see Table IV. Another possible explanation for this delay in the SiF^+ decline is a direct reaction mechanism where the internal and translational degrees of freedom do not fully equilibrate. In such a case, we can determine the magnitude of this delay in the limit that the reaction occurs via an impulsive "pairwise" interaction[63] between Si^+ and SiF_4. This is a more general case of the familiar "spectator stripping" mechanism.[64] In an impulsive process, the reaction is sensitive only to the potential between Si^+ and the F atom transferred. Thus, the energy available to cause chemical change is no longer given in the center-of-mass (c.m.) frame of reference, but in a pairwise frame instead. The conversion of an energy in this pairwise frame of reference to the appropriate energy in the c.m. frame has been derived previously as $E(\text{c.m.}) = E(\text{pair}) \times (A + B)(B + C)/B(A + B + C) = 1.94 \times E(\text{pair})$, where A is the mass of Si^+, B is the mass of F, and C is the mass of SiF_3.[63] For reaction (7a), the pairwise threshold for dissociation will occur at 12.5 eV in the c.m. frame of reference. If the reaction is not strictly impulsive, i.e., the physically realistic situation where there is some interaction between Si^+ and the SiF_3 moiety, then dissociation can occur at lower energies than predicted by the impulsive pairwise model. This clearly must be the case in the present situation.

Process (7b) was discussed earlier as the source for both the decline of the $SiF_3^+ + SiF$ process (2b), and the onset of the second feature in SiF_2^+. Indeed, an analysis of this second feature (after subtracting a model of the lower energy feature and its extrapolation to higher energies) demonstrates that it has a threshold close to 9.1 eV. Also, the SiF_3^+ cross section does peak at approximately E_D [reaction (7b)], which demonstrates that this product retains a considerable fraction of the excess energy. This is again consistent with the fact that SiF_3^+ has more low frequency vibrations than SiF, see Table IV. Also since ground state SiF_3^+ is planar,[51] it may be that when the Si–F bond breaks in tetrahedral SiF_4 to form $SiF_3^+ + SiF$, considerable excess energy could preferentially remain in the umbrella mode of the SiF_3^+. The behavior of $\sigma(SiF_3^+)$ at high energies does not appear to be consistent with an impulsive type of reaction mechanism.

The first feature of $\sigma(SiF_2^+)$, process (2c), also peaks at the thermodynamic limit E_D [reaction (7c)]. Such behavior is consistent with a close-collision mechanism, such as those involving intermediates II and III. Here, the kinetic energy of the reactants is readily converted into a broad distribution of internal and translational degrees of freedom in the products, such that there is a finite probability that some SiF_2^+ molecules will dissociate at all interaction energies above E_D.

Finally, we need to explain the persistence of SiF_3^+ at kinetic energies above 18 eV. One possibility is the formation of excited state products (either of SiF_3^+ or SiF). Another possibility is that this is due to a charge transfer mechanism, process (8)[65]:

$$Si^+ + SiF_4 \rightarrow SiF_4^+ + Si, \quad E_{CT} = 7.5 \text{ eV}, \tag{8a}$$

$$\downarrow$$

$$SiF_3^+ + F + Si, \quad E_{CT} = 8.2 \text{ eV}. \tag{8b}$$

The arrow marked as E_{CT} in Fig. 1 denotes the threshold for the fragmentation process (8b). A cross section function which rises from this threshold [Eq. (3) with $E_T = 8.2$ eV, $n = m = 1$] can account for the SiF_3^+ cross section at the highest energies. The SiF_4^+ product, channel (8a), was not observed. One possible explanation for this is that SiF_4^+ dissociates readily above the threshold for reaction (8b). Indeed, photoionization cross sections for $Si(CH_3)_4$, $SiF(CH_3)_3$, $SiF_2(CH_3)_2$, and $SiF_3(CH_3)$ show that the parent ions undergo the analogous fragmentation processes within 1 eV above the appearance potential of the fragment ion.[48] Thus, it is possible that only at the higher energies, where SiF_3^+ would dominate, do the intensitities of the charge transfer processes exceed our detection sensitivity. We estimate that the cross section for reaction (8a) is less than 0.002 $Å^2$, since the collection efficiency of charge transfer products may be as low 50%, as discussed above.

Molecular orbital correlations and potential energy surfaces

Insight into the dynamics of the interaction of Si^+ and SiF_4 can be obtained by using simple molecular orbital (MO) arguments to develop qualitative potential energy surfaces. In the past, such arguments have been used to explain the reaction dynamics of simple systems involving three or four atoms.[34,66] In larger systems such as the present case, simplifying assumptions can be made which allow the illustration of dominant effects.[67]

For the Si^+ reactant, the ground state is ^2P and has a valence electron configuration of $(3s)^2(3p)^1$. Consider the possible geometries for approach of the Si^+ reactant toward $F\text{–}SiF_3$. If the half-filled $3p(Si^+)$ orbital were directed along an $F\text{–}SiF_3$ bond, severe repulsion between the Si^+ electron and the two electrons within the Si–F bonding orbital would result. This repulsion is clearly reduced if this $3p(Si^+)$ orbital remains empty while the electron is in a $3p(Si^+)$ orbital perpendicular to the $F\text{–}SiF_3$ bond. If the approach is not collinear, then the half-filled $3p(Si^+)$ orbital is bent toward the surrounding F atoms and increased electron–electron repulsion would result. These simple considerations suggest that the lowest-energy approach of the Si^+ and SiF_4 reactants is in C_{3v} symmetry, the collinear geometry, and involves primary interaction of Si^+ with only one of the F atoms on SiF_4. This clearly explains the very small cross section for $SiF_2^+ + SiF_2$ formation, a process which must involve a noncollinear approach.

In order to simplify the following arguments, we will treat the SiF_3–F reactant as a diatomic species AF. Based on the ideas developed in the preceding paragraph, this should be a reasonable approximation. The highest occupied orbitals of AF include the two filled $p\pi(F)$ orbitals, as well as the orbital of the Si–F bond cleaved during reaction, denoted as $\sigma(AF)$. The lowest unoccupied orbital of AF is $\sigma^*(AF)$. The energy of the $p\pi(F)$ and $p(Si)$ orbitals is taken as the ionization potentials of SiF_4 (IP = 15.86 eV) and Si (IP = 8.15 eV), respectively.[68] The energy spacing between the $\sigma(AF)$ and $p\pi(F)$ orbitals (1.5 eV), and the spacing between the $\sigma(AF)$ and $\sigma^*(AF)$ orbitals (26 eV) is estimated by analogy with calculations on the $SiFH_3$ system.[69] Any uncertainty in the exact position of these orbitals is unlikely to affect the qualitative conclusions of the resulting MO diagram. The final ordering of the reactant MOs is shown on the left-hand side of Fig. 4.

For the SiF and SiF^+ products, the valence electron configurations are $(\pi)^4(\sigma)^2(\pi^*)^1$ for the SiF ($^2\Pi_u$) ground state, $(\pi)^4(\sigma)^2(\sigma^*)^1$ for the SiF ($^2\Sigma^+$) first excited state, $(\pi)^4(\sigma)^1(\pi^*)^2$ for the SiF($^4\Sigma^-$) second excited state, and $(\pi)^4(\sigma)^2$ for ground state SiF^+ ($^1\Sigma^+$). The π and π^* orbitals are formed by the overlap of the $3p\pi(Si)$ and $2p\pi(F)$ atomic orbitals, where the π and π^* orbitals have mostly $2p(F)$ and $3p(Si)$ character, respectively. The σ and σ^* orbitals are largely $2p(F)$ and hybridized $3sp(Si)$ orbitals.[1] The energy of the π^* orbital is taken as IP(SiF) = 7.55 eV, and the σ^* energy level comes from the term value for the SiF($^2\Sigma^+$) state (2.8 eV).[39] Likewise the term value of the SiF($^4\Sigma^-$) state (3.7 eV) provides the σ orbital energy level.[39] While the energy of the π(SiF) orbitals is not known, they must lie below the other product orbitals. To estimate the π(SiF) energy level, we assume the π–π^* splitting is equal to the σ–σ^* splitting (6.5 eV). In the A and A^+ products, the only MO of interest is that which remains of the cleaved $\sigma(AF)$ orbital, denoted here by $\sigma(A\cdot)$. Its energy level is determined from the ionization potential of SiF_3 (10.0 eV). The right-hand side of Fig. 4 shows the final ordering and spacing of the product orbitals. Once again, the qualitative conclusions of the MO diagram would be unaffected by small shifts in these energy level spacings.

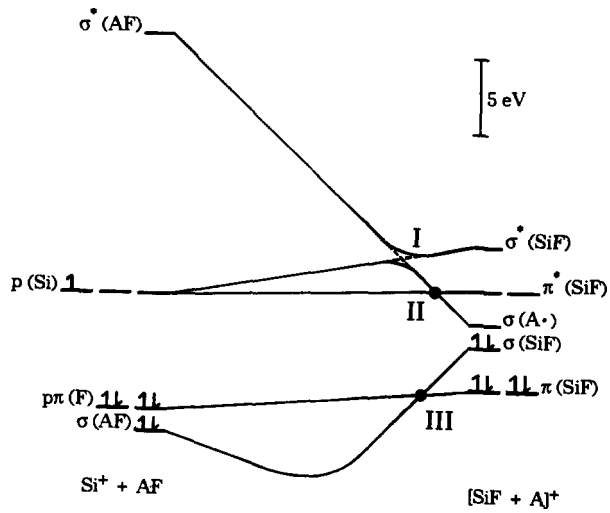

FIG. 4. Qualitative molecular orbital correlation diagram for reactions (2a) and (2b), where A denotes the SiF_3 fragment. The orbital energies (along the vertical axis with the approximate scale shown) are indicated by horizontal lines and are determined as discussed in the text. Roman numerals indicate orbital crossings for reference in the text. At crossing I (which is avoided in all geometries), solid and dashed lines indicate adiabatic and diabatic correlations, respectively. Circles indicate that the crossings become avoided in C_s symmetry.

Having ascertained the ordering of the salient MOs, we now determine the correlation between the reactant and product orbitals. Literature discussions of analogous three-atom systems utilize the nodal structure of the evolving MOs to determine these correlations.[66] The resulting diabatic correlations (i.e., the electron configuration is maintained throughout the reaction) are shown in Fig. 4. Three orbital crossings can be seen. The highest of these, crossing I, involves two σ orbitals and therefore will be avoided in all symmetries. Crossings II and III, however, involve a σ and a π orbital and thus do not interact in $C_{\infty v}$ symmetry. If the symmetry is reduced to C_s, the σ orbital resolves into a', and the π orbitals resolve into a' and a''. Thus, there will be an avoided crossing between the two a' orbitals if the symmetry relaxes from collinear in the exit channel.

From these MO correlations, we now consider the possible electron occupations of the product orbitals. The electrons beginning in the $p\pi(F)$ and $\sigma(AF)$ orbitals flow into σ(SiF) and π(SiF), as required for both reactions (2a) and (2b). Whether crossing III is avoided or not is inconsequential, since all these orbitals are filled. The critical electron, then, is the one in the $p(Si)$ orbital. By examining the possi-

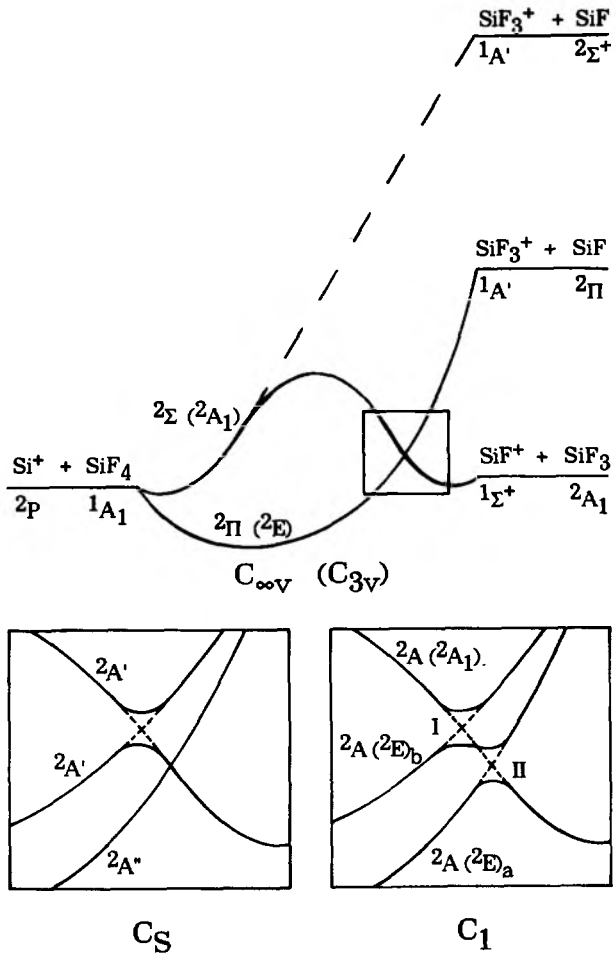

FIG. 5. Qualitative potential energy surfaces for reactions (2a) and (2b) for a collinear approach ($C_{\infty v}$ symmetry in the atom–diatom approximation, or C_{3v} symmetry in general). The region of the surface crossings near the exit channel is shown in C_s symmetry in the first inset. Here, the dashed lines indicate diabatic behavior at the $^2A'$–$^2A'$ surface crossing, while solid lines show adiabatic behavior. The region of the surface crossings is also shown in C_1 symmetry in the second inset. Here, too, dashed lines indicate diabatic behavior at the ^2A–^2A crossings I and II.

ble MO correlations for this electron, qualitative potential energy surfaces are obtained for reactions (2a) and (2b). These are shown in Fig. 5.

As the reactants interact, three doublet surfaces are formed. In our atom–diatom approximation, collinear symmetry in the entrance channel results in a $^2\Pi$ surface and a $^2\Sigma$ surface. If the electron of interest begins in the p(Si) orbital directed along the reaction coordinate [denoted here as $p\sigma$(Si)], there must be a strong repulsion between this electron and the filled σ(AF) orbital. This electron configuration corresponds to the $^2\Sigma$ surface which diabatically correlates with excited products $SiF(^2\Sigma^+) + SiF_3^+(^1A')$, 2.8 eV above the ground state products $SiF(^2\Pi) + SiF_3^+(^1A')$. This surface must undergo an avoided crossing with another $^2\Sigma$ surface such that it adiabatically correlates with ground state products, $SiF^+(^1\Sigma^+) + SiF_3(^2A_1)$, process (2a). This surface crossing corresponds to the orbital crossing I in Fig. 4. Based on these considerations, *we assume that the* $^2\Sigma$ *surface is unreactive.* Alternatively, if the $p\sigma$(Si) orbital is empty, the $p\pi$(Si) electron diabatically correlates with the π^*(SiF) orbital. There are no strong repulsions and therefore we anticipate that the resultant $^2\Pi$ surface will be moderately attractive. This surface diabatically correlates with the $SiF_3^+(^1A') + SiF(^2\Pi)$ product channel, process (2b). Clearly, the $^2\Pi$ and $^2\Sigma$ surfaces must cross, Fig. 5, and this corresponds to crossing II in the MO correlation diagram, Fig. 4. Qualitatively, the same surfaces are obtained if we consider the full C_{3v} symmetry of the Si^+–F–SiF_3 collinear approach. In this symmetry, the repulsive $^2\Sigma$ surface becomes a $^2A_1$ surface, and the $^2\Pi$ surface becomes a ^2E surface,[70] and they again cross one another.

Since reaction (2a) is observed to occur at the thermodynamic threshold with no activation barrier, there *must* be mixing of the Π (E) and Σ (A_1) surfaces. This can occur if the Si–F–Si angle deviates from 180° in the exit channel, resulting in lower symmetry at the surface crossing. In the atom–diatom approximation, such geometries have C_s symmetry. The $^2\Sigma$ surface becomes $^2A'$, and the $^2\Pi$ surface splits into $^2A'$ and $^2A''$. The $^2A''$ surface corresponds to the half-filled $p\pi$(Si) orbital directed out of the plane of symmetry, which results in less repulsion between the Si electron and those of species A. Thus, this surface lies lower in energy than the $^2A'$ surface, in which the $p\pi$(Si) orbital lies in the plane of symmetry. The region of the surface crossings in C_s symmetry is shown in an inset in Fig. 5. The $^2A'$–$^2A'$ crossing is avoided, and $SiF^+ + SiF_3$ can be formed along the lowest surface. Since reaction (2a) is observed at the thermodynamic threshold, there must be no barrier in excess of the threshold along this surface. Since the $^2A''$–$^2A'$ crossing is not avoided, the $^2A''$ surface correlates only with the $SiF_3^+ + SiF$ channel.

If we now consider the real symmetry of reaction, the most general configuration for the exit channel has C_1 symmetry. [There are, however, six configurations of C_s symmetry where the Si–F–(SiF_2)–F angles are coplanar.] In C_1 symmetry, all three surfaces are ^2A and are shown at the region of the surface crossings in a second inset in Fig. 5. The lowest ^2A surface originates as ^2E and is denoted here as $^2A(^2E)_a$. This surface avoids crossing $^2A(^2A_1)$ at II and thus correlates to the $SiF^+ + SiF_3$ channel (2a). Likewise, the $^2A(^2A_1)$ surface avoids crossing I with the $^2A(^2E)_b$ surface, and correlates with the $SiF_3^+ + SiF_3$ channel (2b). Last, the avoided crossing at I initially correlates the $^2A(^2E)_b$ surface with channel (2a). However, crossing II is also avoided, and so this surface ultimately correlates with the $SiF_3^+ + SiF$ channel (2b).

Therefore, qualitative results for the most general case are the same as those where the interaction is in C_s symmetry. In particular, process (2a) can occur at threshold along one of the low-energy surfaces if the reaction geometry is noncollinear. Reaction (2b) can occur at threshold along the second low-energy surface in any geometry. This adiabatic behavior is sufficient to explain the gross features of the experimental results, but adiabatic behavior alone does not explain the observed competition between these two reaction channels.

SiF^+ and SiF_3^+ competition

As mentioned in the Results section, reactions (2a) and (2b) appear to compete directly with one another, as evi-

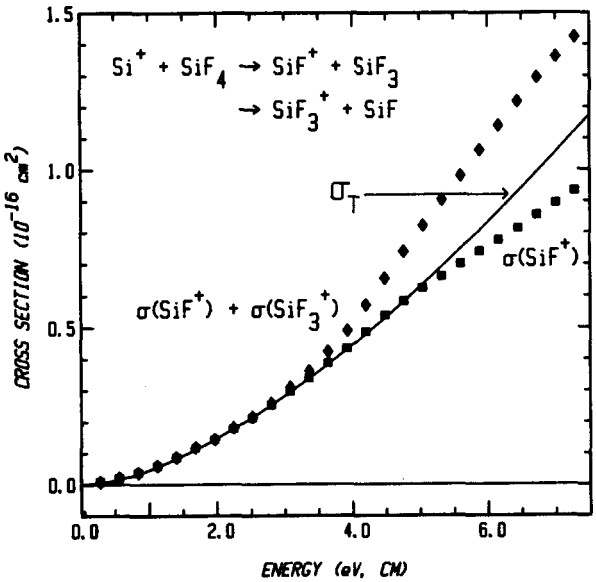

FIG. 6. Product ion cross sections from reactions (2a) and (2b) as a function of translational energy in the center-of-mass frame (lower scale). The solid line shows the convoluted threshold fit σ_T of channel (2a, squares), with $m = 1$, $n = 2.5$, and $E_T = 0.10$ eV. The sum of channels (2a) and (2b) is given by the solid diamonds.

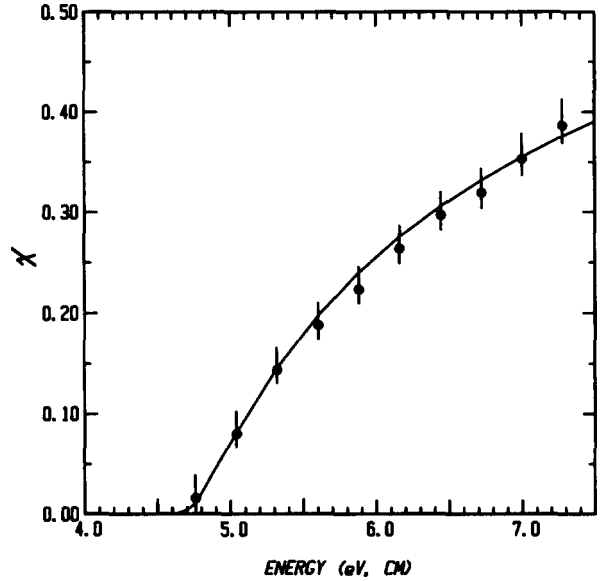

FIG. 7. Fraction χ of $SiF_3^+ + SiF$, channel (2b), produced in competition with $SiF^+ + SiF_3$, channel (2a), as a function of relative translational energy. Circles show χ obtained using the threshold model Eq. (3) with $m = 1$ as described in the text. Error limits are determined by using Eq. (3) with $m = 0$ and 3. The line shows the calculated Landau–Zener probability, Eq (9), with $B = 1.6$ and $E_x = 4.6$.

denced by the break in $\sigma(SiF^+)$ at ~ 5 eV. If SiF^+ and SiF_3^+ production were in direct competition, then we might expect that a single, general threshold function σ_T would describe the sum of these two channels (until an energy where dissociation processes become significant). Below 2 eV, $\sigma(SiF_3^+)$ is zero, and thus σ_T must be equivalent to the threshold fit for the SiF^+ channel alone. Figure 6 shows the SiF^+ reaction channel, the sum of the SiF^+ and SiF_3^+ channels, and the threshold fit σ_T of $\sigma(SiF^+)$ using Eq. (3) with $m = 1$, $n = 2.5$, and $E_T = 0.10$ eV. (The $m = 0$ and $m = 3$ models are nearly identical.) Comparison of σ_T to the SiF^+ channel alone clearly depicts the break in the cross section function at 5 eV. Yet the sum of SiF^+ and SiF_3^+ is significantly larger than σ_T above ~ 4 eV. To the degree that σ_T is a valid representation of the competing channels, this implies that only a fraction χ of the total SiF_3^+ observed is produced by a mechanism in direct competition with SiF^+, as indicated in Eq (5):

$$\sigma(SiF^+) + \chi\sigma(SiF_3^+) = \sigma_T. \quad (5)$$

χ can be readily solved for, and in Fig. 7, χ is plotted as a function of energy for the three threshold fits considered ($m = 0$, 1, 3). For these models, χ is zero below 4.6 ± 0.2 eV, rises monotonically, and gradually begins to level out. At energies above ~ 7.5 eV, χ cannot be reasonably evaluated due to the influence of dissociation processes.

By considering both the adiabatic and diabatic character of the surfaces shown in Fig. 5, this energy dependent competition can be qualitatively explained. In the interests of clarity, we will use the C_s symmetry designations for the surfaces, although the results are unchanged for the more general case of C_1 symmetry. We also assume that the $^2A'(^2\Sigma)$ surface is completely unreactive. Note that the $^2A''$ surface is a source for SiF_3^+ which does not compete with SiF^+ production, and therefore it is not surprising that the sum of $\sigma(SiF^+)$ and $\sigma(SiF_3^+)$ is not accurately modeled by σ_T. The observed competition between processes (2a) and (2b) must involve the behavior at the interaction of the $^2A'$ surfaces. If the behavior at the avoided crossing were always diabatic (i.e., SiF_3^+ is formed), then the fraction of $\sigma(SiF_3^+)$ in direct competition with $\sigma(SiF^+)$, χ, would be one-half. On the other hand, if the behavior were exclusively adiabatic (i.e., SiF^+ is formed), then χ would be 0. As is evident in Fig. 7, χ spans this range of values as the interaction energy is increased. Thus, χ is a rough indication of the extent of diabatic behavior at the avoided crossing of the A'–A' surfaces. There may be an enhanced propensity for diabatic behavior in this system, because the diabatic behavior in C_s (C_1) symmetry is equivalent to adiabatic behavior of the $^2A_1$ and ^2E surfaces in the C_{3v} symmetry of the favored collinear geometry, Fig. 5.

As is clear from Fig. 7, χ varies with kinetic energy such that the behavior becomes increasingly diabatic as the energy is increased. One simple theory which predicts such an energy dependence in the competition between adiabatic and diabatic behavior is the Landau–Zener (LZ) model.[71] This model treats the case of a particle moving with constant velocity v along a potential energy surface near an avoided surface crossing. The velocity is related to the kinetic energy of the particle E and the potential energy at the crossing point E_x, such that $v = [2(E - E_x)/\mu]^{0.5}$. The probability of diabatic behavior during a single pass through the crossing region is given in Eq. (9):

$$P \propto \exp(-B'/v) = \exp[-B/(E - E_x)^{0.5}], \quad (9)$$

where B' is the coupling strength between the two surfaces. This function is shown in Fig. 7 for the values $B = 1.6$ and $E_x = 4.6$, and can be seen to be a very reasonable representation of χ. We hesitate to place too much emphasis on the physical interpretation of these values for B and E_x, because the potential energy surfaces of reaction (2) are far more complex than that considered in the LZ model.[72] Nevertheless, some comment is probably in order on the origin of the apparent 4.6 eV "threshold" for competition between reactions (2a) and (2b). This is clearly well above the thermodynamic threshold for the $SiF_3^+ + SiF$ channel, 2.48 ± 0.14 eV. It may, however, be related to the pairwise threshold for this channel, 4.8 ± 0.3 eV.[63] This would imply that the competition occurs when the system is behaving impulsively, a situation which plausibly would favor diabatic behavior.

SUMMARY

Guided ion beam mass spectrometry has been used to study the reaction of Si^+ with SiF_4. No reaction occurs at thermal energies, consistent with a previous study of this reaction,[3] but at elevated energies, several product ions are observed, SiF^+, SiF_2^+, and SiF_3^+, but no $Si_2F_x^+$ species. All three reaction channels are endothermic, and analysis of the cross sections results in threshold energies of 0.10 ± 0.05, 2.35 ± 0.12, and 2.48 ± 0.14 eV, respectively. This energetic information is then used to derive thermochemistry for SiF_x and SiF_x^+ species. Literature values are reevaluated in light of the present work, and recommended heats of formation and ionization potentials are compiled in Tables II and III. One major change recommended to the literature values involves $\Delta H_f^0(SiF_3)$, for which values conflicting by 20 kcal /mol have recently been reported.[39,40] Here we recommend the value -258 ± 3 kcal/mol. Another major amendment to the literature is $IP(SiF) = 7.54 \pm 0.16$ eV, which involves a change of 0.28 eV from the previously accepted value.[46]

The results of phase space theory calculations[57] and the threshold modeling indicate that the SiF^+ and SiF_3^+ products are produced primarily by a direct interaction between Si^+ and one fluorine atom on SiF_4. SiF_2^+ must presumably be formed instead through a hindered mechanism, possibly insertion. A second major process which produces SiF_2^+ is dissociation of the SiF_3^+ product ion.

Simple molecular orbital arguments are applied here to gain insight into the dynamics of SiF^+ and SiF_3^+ production and the competition of the SiF and SiF_3 species for the odd electron. Resulting potential energy surfaces show that production of SiF_3^+ alone occurs on one surface, and competition between the SiF^+ and SiF_3^+ channels occurs along another surface. This latter surface correlates diabatically with $SiF_3^+ + SiF$ and adiabatically with $SiF^+ + SiF_3$. The observed energy dependence of diabatic vs adiabatic behavior concurs with that given in the simple Landau–Zener formalism.[71]

ACKNOWLEDGMENT

This work was funded by the National Science Foundation, Grant No. CHE-8796289.

[1] B. J. Garrison and W. A. Goddard III, J. Chem. Phys. **87**, 1307 (1987).
[2] (a) T. R. Hayes, R. C. Wetzel, F. A. Baiocchi, and R. S. Freund, J. Chem. Phys. **88**, 823 (1988); (b) T. R. Hayes, R. S. Shul, S. A. Baiocchi, R. C. Wetzel, and R. S. Freund, *ibid.* (submitted).
[3] W. D. Reents, Jr. and A. M. Mujsce, Int. J. Mass Spectrom. Ion Process. **59**, 65 (1984).
[4] S. N. Senzer and F. W. Lampe, J. Appl. Phys. **54**, 3524 (1982).
[5] A. Madan and S. R. Ovshinsky, J. Non-Cryst. Solids, **35/36**, 171 (1980).
[6] For a thorough review of plasma etching see (a) J. A. Mucha and D. W. Hess, Am. Chem. Soc. Symp. **219**, 215 (1983); (b) D. L. Flamm and V. M. Donnelly, Plasma Chem. Plasma Process. **1**, 317 (1981); J. W. Coburn, *ibid.* **2**, 1 (1982).
[7] Y. Matsumi, S. Toyoda, T. Hayashi, M. Miyamura, H. Yoshikawa, and S. Komiya, J. Appl. Phys. **60**, 4102 (1986).
[8] D. L. Flamm, V. M. Donnelly, and J. A. Mucha, J. Appl. Phys. **52**, 3633 (1981).
[9] P. A. Longeway, R. D. Estes, and H. A. Weakliem, J. Phys. Chem. **88**, 73 (1984).
[10] G. C. Schwartz and P. M. Shaible, J. Vac. Sci. Technol. **16**, 410 (1979).
[11] T. D. Mantei, J. Electrochem. Soc. **130**, 1958 (1983).
[12] N. May, U. Carmi, I. Rosenthal, R. Avni, R. Manory, and A. Grill, J. Appl. Phys. **55**, 4404 (1984).
[13] C. A. DeJoseph, Jr., P. D. Haaland, and A. Garscadden, IEEE Trans. Plasma Sci. **PS-14**, 165 (1986).
[14] I. Haller, in *Proceedings of the 6th International Conference on Plasma Chemistry*, edited by M. I. Boulos and R. J. Munz (Montreal, Canada, 1983), Vol. 3, p. 826.
[15] G. Turban, Y. Catherine, and B. Grolleau, Plasma Chem. Plasma Process. **2**, 61 (1982); Thin Solid Films **67**, 309 (1980).
[16] J. Perrin, J. P. M. Schmitt, G. deRosny, B. Drevillon, J. Huc, and A. Lloret, J. Chem. Phys. **73**, 383 (1982).
[17] H. Chatham and A. Gallagher, J. Appl. Phys. **58**, 159 (1985).
[18] R. Manory, A. Grill, U. Carmi, and R. Avni, Plasma Chem. Plasma Process. **3**, 235 (1983).
[19] M. L. Mandich, W. D. Reents, Jr., and M. F. Jarrold, J. Chem. Phys. **88**, 1703 (1988); K. Raghavachari, *ibid.* **88**, 1688 (1988); W. D. Reents, Jr. and M. L. Mandich, J. Phys. Chem. (submitted).
[20] For a recent review see G. Turban, Pure Appl. Chem. **56**, 215 (1984).
[21] For a review of endpoint detection methods see P. J. Marcoux and P. W. Foo, Solid State Technol. **24**, 115 (1981).
[22] A. Garscadden, in *Plasma Processing*, edited by J. W. Coburn, R. A. Gottscho, and D. W. Hess, MRS Symposia Proceedings (Materials Research Society, Pittsburgh, 1986), Vol. 68, p. 127; M. J. Kushner, in *Plasma Processing*, edited by J. W. Coburn, R. A. Gottscho, and D. W. Hess, MRS Symposia Proceedings (Materials Research Society, Pittsburgh, 1986), Vol. 68, p. 293.
[23] J. E. Nicholas and A. I. Spiers, Plasma Chem. Plasma Process. **5**, 263 (1985).
[24] R. A. Gottscho, G. P. Davis, and R. H. Burton, Plasma Chem. Plasma Process. **3**, 193 (1983).
[25] P. Briaud, G. Turban, and B. Grolleau, in *Plasma Processing*, edited by J. W. Coburn, R. A. Gottscho, and D. W. Hess, MRS Symposia Proceedings (Materials Research Society, Pittsburgh, 1986), Vol. 68, p. 109.
[26] For instance, recommended values for $\Delta H_f^0(SiF_3)$ range from -239 to -259 kcal/mol (Ref. 40).
[27] B. H. Boo and P. B. Armentrout, J. Am. Chem. Soc. **109**, 3549 (1987).
[28] J. L. Elkind and P. B. Armentrout, J. Phys. Chem. **88**, 5454 (1984).
[29] B. H. Boo and P. B. Armentrout, J. Phys. Chem. **91**, 5777 (1987).
[30] K. M. Ervin and P. B. Armentrout, J. Chem. Phys. **83**, 166 (1985).
[31] E. Teloy and D. Gerlich, Chem. Phys. **4**, 417 (1974).
[32] The isotopic abundance of ^{28}Si is 92.23%, ^{29}Si is 4.67%, and ^{30}Si is 3.10%.
[33] P. M. Hierl, V. Pacak, and Z. Herman, J. Chem. Phys. **67**, 2678 (1977).
[34] J. L. Elkind and P. B. Armentrout, J. Phys. Chem. **91**, 2037 (1987).
[35] C. E. Moore, Natl. Stand. Ref. Data Ser. (U. S. Natl. Bur. Stand.) **34** (1970).
[36] K. M. Ervin and P. B. Armentrout, J. Chem. Phys. **84**, 6738 (1986).
[37] N. Aristov and P. B. Armentrout, J. Am. Chem. Soc. **108**, 1806 (1986); L. Sunderlin, N. Arisotov, and P. B. Armentrout, *ibid.* **109**, 78 (1987).
[38] W. J. Chesnavich and M. T. Bowers, J. Phys. Chem. **83**, 900 (1979).
[39] M. W. Chase, Jr., C. A. Davies, J. R. Downey, Jr., D. J. Frurip, R. A. McDonald, and A. N. Syverud, *JANAF Thermochemical Tables*, 3rd ed., J. Phys. Chem. Ref. Data **14**, Suppl. 1 (1985).
[40] R. Walsh, J. Chem. Soc. Faraday Trans. 1 **79**, 2233 (1983).
[41] V. L. Talrose, P. S. Vinogradov, and I. K. Larin, in *Gas Phase Ion Chemistry*, edited by M. T. Bowers (Academic, New York, 1979), p. 305.

[42]T. C. Ehlert and J. L. Margrave, J. Chem. Phys. **41**, 1066 (1964).
[43]M. Farber and R. D. Srivastava, J. Chem. Soc. Faraday Trans. 1 **74**, 1089 (1978).
[44]M. E. Weber and P. B. Armentrout (work in progress).
[45]M. Farber and R. D. Srivastava, J. Chem. Phys. **81**, 241 (1984). The value and uncertainty given here is from the average of $\Delta H_f^0(BF_2)$ obtained from studies of BF_3 thermal dissociation, photoionization, and the reactions of BF_3 with B and B_2O_3.
[46]J. W. C. Johns and R. F. Barrow, Proc. Phys. Soc. (London) **71**, 476 (1958).
[47]J. D. McDonald, C. H. Williams, J. C. Thompson, and J. L. Margrave, Adv. Chem. Ser. **72**, 261 (1968).
[48]M. K. Murphy and J. L. Beauchamp, J. Am. Chem. Soc. **99**, 2085 (1977).
[49]This value differs from that reported by Murphy and Beauchamp (Ref. 48), -22.7 kcal/mol. It is instead calculated with $\Delta H_f^0(CH_3) = -34.82 \pm 0.19$ kcal/mol (Ref. 39) and is converted from the stationary electron convention.
[50]G. E. P. Box, W. G. Hunter, and J. S. Hunter, *Statistics for Experimenters* (Wiley, New York, 1978), p. 319.
[51]M. O'Keeffe, J. Am. Chem. Soc. **108**, 4341 (1986).
[52]A. M. Doncaster and R. Walsh, Int. J. Chem. Kinet. **13**, 503 (1981).
[53]Isodesmic reactions involve reactants and products which contain the same numbers and types of bonds.
[54]H. B. Schlegel, J. Phys. Chem. **88**, 6254 (1984).
[55]N. P. C. Westwood, Chem. Phys. Lett. **25**, 558 (1974).
[56]T. P. Fehlner and D. W. Turner, Inorg. Chem. **13**, 754 (1974).
[57](a) W. J. Chesnavich and M. T. Bowers, J. Chem. Phys. **68**, 901 (1978); **66**, 2306 (1977); D. A. Webb and W. J. Chesnavich, J. Phys. Chem. **87**, 3791 (1983); (b) J. C. Light and J. Lin, J. Chem. Phys. **43**, 3209 (1965); (c) E. E. Nikitin, Teor. Eksp. Khim. **1**, 135, 144, 248 (1965) [Theor. Exp. Chem. (Eng. Trans.) **1**, 83, 90, 275 (1975)].
[58]M. E. Weber, J. L. Elkind, and P. B. Armentrout, J. Chem. Phys. **84**, 1521 (1986); K. M. Ervin and P. B. Armentrout, *ibid.* **84**, 6750 (1986); J. D. Burley, K. M. Ervin, and P. B. Armentrout, Int. J. Mass Spectrom. Ion Proc. **80**, 153 (1987).
[59]M. E. Grice, K. Song, and W. J. Chesnavich, J. Phys. Chem. **90**, 3503 (1986).
[60]G. Gioumousis and D. P. Stevenson, J. Chem. Phys. **29**, 294 (1958).
[61]M. L. Mandich, W. D. Reents, Jr., and M. F. Jarrold, J. Chem. Phys. (submitted).
[62]Average bond energies are calculated by using the data and method of Margrave and co-workers (Ref. 47). Here, however, $\Delta H_f^0(Si_2F_6)$ and $\Delta H_f^0(Si_3F_8)$ are calculated using their data in conjunction with the recommended thermochemistry in Table III, and all SiF_x and SiF_x^+ species are used to calculate the average silicon–fluorine bond energy.
[63]J. L. Elkind and P. B. Armentrout, J. Chem. Phys. **84**, 4862 (1986).
[64]A. Henglein and K. Lacmann, Adv. Mass Spectrom. **3**, 331 (1966); A. Henglein, in *Ion–Molecule Reactions in the Gas Phase*, edited by P. J. Ausloos (American Chemical Society, Washington, D. C., 1966), p. 63; A. Ding, K. Lacmann, and A. Henglein, Ber. Bunsenges. Phys. Chem. **71**, 596 (1967).
[65]E_{CT} for process (6a) is calculated from IP(SiF_4) in Ref. 68.
[66]B. H. Mahan, J. Chem. Phys. **55**, 1436 (1971); Acc. Chem. Res. **8**, 55 (1975).
[67]R. Georgiadis and P. B. Armentrout, J. Am. Chem. Soc. **108**, 2119 (1986); N. Arisotov and P. B. Armentrout, J. Phys. Chem. **91**, 6178 (1987).
[68]H. M. Rosenstock, K. Draxl, B. W.Steiner, and J. T. Herron, J. Phys. Chem. Ref. Data **6**, Suppl. 1 (1977).
[69]R. F. Hout, Jr., W. J. Pietro, and W. J. Hehre, *A Pictorial Approach to Molecular Structure and Reactivity* (Wiley, New York, 1984), p. 88.
[70]In C_{3v} symmetry, the reactants Si^+ (^2P_u) and SiF_4 ($^1A_1$) resolve into $^2A_1 + {}^2E$ and $^1A_1$, respectively, which leads to $^2A_1$ and ^2E surfaces. The SiF^+ ($^1\Sigma^+$) and SiF_3 ($^2A_1$) product channel (2a) resolves into $^1A_1$ and $^2A_1$ species, and thus a $^2A_1$ surface. Lastly, the SiF_3^+ ($^1A_1$) and SiF($^2\Pi$) product channel (2b) resolves into $^1A_1$ and ^2E species, yielding ^2E surfaces. See G. Herzberg, *Molecular Spectra and Molecular Structure. III. Electronic Spectra of Polyatomic Molecules* (Van Nostrand Reinhold, New York, 1966), p. 570; I. W. M. Smith, *Kinetics and Dynamics of Elementary Gas Reactions* (Butterworths, London, 1980), p. 50.
[71]L. D. Landau, Phys. Z. Sowjetunion **2**, 46 (1932); C. Zener, Proc. R. Soc. London Ser. A **137**, 696 (1932); E. C. G. Stueckelberg, Helv. Phys. Acta **5**, 369 (1932).
[72]R. H. Schultz and P. B. Armentrout, J. Phys. Chem. **91**, 4433 (1987).